Polymerization of tetrahydrofurfuryl methacrylate in three-component anionic microemulsions

ARTICLE *in* MACROMOLECULES · SEPTEMBER 1992

Impact Factor: 5.8 · DOI: 10.1021/ma00046a007

Polymerization of Tetrahydrofurfuryl Methacrylate in Three-Component Anionic Microemulsions

A. P. Full, J. E. Puig,† L. U. Gron,‡ and E. W. Kaler*

Department of Chemical Engineering, University of Delaware, Newark, Delaware 19716

J. R. Minter,§ T. H. Mourey,‖ and J. Texter*,⊥

Imaging Research Laboratories and Analytical Technology Division, Eastman Kodak Company, Rochester, New York 14650

Received February 7, 1992; Revised Manuscript Received May 26, 1992

ABSTRACT: Tetrahydrofurfuryl methacrylate (THFM) polymerizes at 60 °C when initiated with potassium persulfate in three-component microemulsions made with Aerosol-OT (AOT) and water. The resulting monodisperse microlatex contains particles with mean diameters from 25 to 34 nm and polymer molecular weights of order 10^7. Each particle consists of approximately one polymer molecule in a collapsed state. Polymerization kinetics are followed by calorimetry, dilatometry, and internal reflectance infrared spectroscopy. Reaction rate curves show two intervals only: an interval of increasing rate immediately followed by an interval of decreasing rate. Weight-average molecular weight as measured by size-exclusion chromatography and particle size as measured by quasielastic light scattering increase during polymerization. Transmission electron microscopy (TEM) shows the in situ formation of lamellar and multilamellar structures when excess AOT from micelles depleted of monomer exceeds its solubility in water. These findings confirm that latex particles grow by recruiting monomer from uninitiated microemulsion droplets.

Introduction

Emulsion, miniemulsion, and, more recently, microemulsion polymerization are processes that can produce polymeric particles of large molecular weights (10^5 to 10^7) and small sizes (10–1000 nm) dispersed in aqueous (or nonaqueous) media.[1-4] In these processes fast reaction rates and large molecular weights can be achieved simultaneously because free radicals that initiate and propagate the reaction are isolated in small loci.[1,3,4] Microemulsions, in contrast to emulsions and miniemulsions, are thermodynamically stable, transparent dispersions of oil and water, although larger amounts of surfactant and often an alcohol cosurfactant are required for their formation.[4]

Monomers have been polymerized in oil-in-water (o/w), water-in-oil (w/o) and bicontinuous microemulsions.[5-15] Although the simplest microemulsion contains only three components (water, monomer, and pure surfactant), most formulations require cosurfactants or salt to achieve stability, thus increasing the number of components to four or five. However, kinetic data from three-component systems are easier to analyze since the effects of alcohol cosurfactants, which are known to modify the partitioning of monomers and promote chain-transfer reactions, are eliminated.[6,16]

The first polymerizaton of a three-component microemulsion was reported by Murtagh et al.[12] They polymerized styrene solubilized in rodlike micellar solutions of cetyltrimethylammonium bromide (CTAB) to produce latexes with diameters from 11 to 56 nm. Our group polymerized styrene in three-component microemulsions made with the cationic surfactant dodecyltrimethylammonium bromide (DTAB) to produce monodisperse latexes with spherical particles of about 20–31 nm in diameter.[14] More recently, Texter et al.[15] polymerized tetrahydrofurfuryl methacrylate (THFM) in a three-component anionic microemulsion stabilized with Aerosol OT (AOT) using redox initiation and produced crosslinked, monodisperse particles roughly 70 nm in diameter. In the AOT/THFM/water system, smaller amounts of surfactant are required to form microemulsions than in styrene systems of comparable monomer content.

Here we investigate the polymerization of THFM in three-component AOT microemulsions at 60 °C using potassium persulfate as initiator. Polymerization kinetics are studied using calorimetry, dilatometry, gravimetry, and internal reflectance infrared spectroscopy. Quasielastic light scattering, size-exclusion chromatography, and transmission electron microscopy provide evidence of growth during polymerization from initiated microemulsion droplets to particles with final diameters of 15–45 nm. These experimental findings provide insight into the mechanism of microemulsion polymerization and the evolution of latex microstructure.

Experimental Section

Reagent grade tetrahydrofurfuryl methacrylate (THFM) from Scientific Polymer Products was passed through a DHR-4 column (SPP) to remove the inhibitor. AOT [sodium bis(2-ethylhexyl)-sulfosuccinate] from Fluka with a quoted purity of greater than 98% was used as received. Purification of AOT[17] did not change its surface tension in aqueous solution nor its phase behavior with water and THFM. AIBN (2,2′-azobis[isobutyronitrile]) from ICN Biomedical was purified by dissolving in chloroform, filtering, then precipitating with excess methanol, and recovering AIBN on a filter. Potassium persulfate (98% from MCB Manufacturing Chemist), hydroquinone (99% from Aldrich), methanol (99.9% from Fisher), toluene (Fisher), and tetrahydrofuran (THF, uninhibited HPLC-grade from J. T. Baker) were used as received. Samples were made with distilled and deionized water.

The single-phase o/w microemulsion regions at 25 and 60 °C were determined visually by titrating aqueous preparations of AOT with THFM. Phase boundaries of the oil-rich regions were determined similarly by titrating solutions of AOT in THFM with water. Phase boundaries were checked by preparing samples by weight with compositions below and above the phase bound-

* To whom correspondence should be addressed.
† Visiting Professor, Facultad de Ciencias Químicas, Universidad de Guadalajara, Mexico.
‡ Center for Catalytic Science and Technology, Department of Chemical Engineering, University of Delaware.
§ Analytical Technology Division, 14652-3712.
‖ Analytical Technology Division, 14650-2136.
⊥ Imaging Research Laboratories, 14650-2109.

0024-9297/92/2225-5157$03.00/0

aries determined by titration. Because small amounts of polymer can substantially reduce the size of one-phase microemulsion regions,[18] phase diagrams were determined with THFM as received (i.e., with a few ppm of inhibitor) to inhibit thermal polymerization. Samples were examined through cross polarizers to check for streaming and static birefringence. The lamellar phase was confirmed by examination of samples with a Leitz polarizing microscope.

THFM polymerization was done at 60 °C in a 1-L glass reactor, a 45-mL calibrated dilatometer, a Mettler RC1 calorimeter, and a solution FTIR spectrometer (Spectra-Tech ReactIR). In all experiments microemulsions were initiated with an appropriate volume of a concentrated $K_2S_2O_8$ aqueous solution such that the amount of initiator was 1% (w/w) with respect to monomer. In the 1-L glass reactor, 750 mL of the microemulsion was loaded and heated to 60 °C before adding the initiator. The reacting system was continuously stirred and sparged with argon. During the first minutes of reaction, samples (ca. 15 mL) for gravimetric analysis, size-exclusion chromatography (SEC), and quasielastic light scattering (QLS) were withdrawn every minute using a 20-mL glass syringe, quenched with hydroquinone and put in an ice bath for further inhibition of the reaction. Samples were taken more frequently when the microemulsion became bluish, indicating the onset of the propagation reaction. The polymer was precipitated with methanol, filtered, and dried in a vacuum oven at 50 °C for 24 h.

When the reaction was followed by dilatometry, the microemulsion in the 45-mL calibrated dilatometer was sparged with argon at 60 °C for about 45 min before injecting the initiator solution through a septum. Conversion was proportional to changes in liquid height in the capillary tube of the dilatometer. The dilatometer was calibrated by comparing changes in the capillary height with conversion curves obtained by gravimetry.

Calorimetry was done using a Mettler RC1 calorimeter with a 2-L glass reactor. The reactor was initially filled with 988 g of microemulsion and sparged with nitrogen for 10 min at 25 °C. The reactor was then heated to 60 °C at 1 °C/min, during which time the heat capacity of the charged reactor system was determined. A baseline was determined at 60 °C, and the heat-transfer coefficient for heat flow through the reactor wall was determined by adding a known amount of heat to the reactor and determining the surface area of reagents in contact with the reactor wall. After baseline calibration, the initiator solution was added. The reaction rate was obtained from the power flow and the heat of reaction. The power was calculated from the product of the heat-transfer coefficient, U (W/(m^2/K)), the reactor wall area in contact with reagents, and the measured temperature rise during the reaction. This power was also corrected by a heat capacity term obtained as the product of reagent mass, heat capacity, and temperature rise in the reactor.

Gas chromatographic analysis of the microemulsion and latex for monomer (THFM) and AOT was performed using a Hewlett Packard 5890A gas chromatograph with an HP 7673A autosampler (injector). A flame ionization detector at 340 °C was used with a split/splitless injector in the split mode at 40 mL/min and 200 °C. A 40–300 °C program at 20 °C/min was used with helium as the carrier at 12 psi on a J & W DB-5 15 column (0.32-μm i.d, 1.0-mm film thickness, FSOT capillary). The injector used 1-μL samples. HP 33665 MS-DOS Chemstation software was used for integrating peak areas. Samples were prepared using acetone as solvent. Standard solutions of THFM were used to calibrate the THFM response. Dilutions of $^1/_{10}$, $^1/_{100}$, and $^1/_{1000}$ of a 7.98-mg THFM sample in 4-mL of acetone solution were used for calibration. The AOT response was calibrated using acetone dilutions of 6% (w/w) aqueous AOT solution. Samples were prepared by weighing 100 mg of material to the nearest 0.01 mg and diluting with 4 mL of acetone.

For the solution FTIR experiments, about 60 mL of microemulsion was loaded into a glass reactor with a stainless steel base incorporating a ZnSe crystal for internal reflectance infrared spectroscopy. The solution was degassed with argon for 15 min and heated to 60 °C with continuous stirring. After the initiator was injected, IR spectra were taken from 750–4000 cm^{-1} at 1-min intervals by adding 64 scans at a resolution of 8 cm^{-1}. Kinetic data were extracted from the reaction spectra using the ReactIR series 3.0 Quantitative Analysis software.

QLS measurements were made with equipment previously described.[19] The magnitude of the scattering vector, $q = (4\pi n/\lambda_0) \sin(\theta/2)$, was varied by changing the scattering angle, θ, from 30 to 120°. Here n is the index of refraction and λ_o (488 nm) is the wavelength of the light in vacuum. Intensity correlation data from the homodyne experiment were analyzed by the method of cumulants to provide the average decay rate, $\langle\Gamma\rangle$ ($=q^2D$), where D is the diffusion coefficient, and the normalized variance, ν ($= [(\langle\Gamma^2\rangle - \langle\Gamma\rangle^2)/\langle\Gamma\rangle^2]$, which is a measure of the width of the distribution of the decay rates. The measured diffusion coefficients were represented in terms of apparent radii by using Stokes law and assuming the solvent has the viscosity of water. Latexes were diluted up to 500 times to minimize particle–particle interactions and filtered through 0.2-μm Millex Millipore filters to eliminate dust particles before QLS measurements.

The SEC system using coupled low-angle laser light scattering (LALLS), differential viscometry (DV), and differential refractive index (DRI) detectors was configured as described previously.[20,21] Narrow molecular weight distribution polystyrene standards were obtained from Polymer Laboratories, Inc. Isolated polyTHFM samples were kept under 0.1 mm Hg vacuum at room temperature for 24 h before dissolving at a concentration of 0.5–0.6 mg/mL in THF. All sample solutions were filtered through a 0.5-μm Millex-SR Millipore filter before injecting 100 μL of each sample into the SEC.

Direct images of vitrified thin films of the polymerized microemulsions were recorded at −175 °C in a Phillips CM-12 transmission electron microscope equipped with a Gatan Model 626 cryotransfer holder. Thin liquid films were prepared at 100% relative humidity and 25 °C within a controlled environmental vitrification system (CEVS) similar to that described elsewhere.[15,22] A 7-μL microemulsion droplet was placed on a carbon-coated cellulose acetate butyrate film containing holes 8–10 μm in diameter.[23] Most of the fluid was removed from the grid by blotting with filter paper to produce thin, biconcave menisci of fluid spanning the holes in the grid. The controlled environment of the CEVS prevented loss of volatile species from the film. Immediately after cessation of blotting, a shutter in the bottom of the CEVS was opened and the tweezers containing the specimen were plunged into liquid ethane just above its freezing point. The cooling rates in these thin films are sufficient to prevent crystallization of water, resulting in a vitreous sample. Each grid was placed in liquid nitrogen for storage until it was transferred to the Gatan 626 holder and inserted into the electron microscope for imaging. The specimen temperatures never exceeded −160 °C, which is below −140 °C, the devitrification temperature of water.[24]

Results

The AOT/water/THFM system at 25 °C has rich phase behavior (Figure 1a). There are three highly viscous one-phase mesomorphic regions: lamellar (L_α), inverse cubic (I_2) and inverse hexagonal (H_2). L_α samples are birefringent and show characteristic oily streaks and maltese crosses when observed with a polarizing optical microscope.[25] There are, in addition, two isotropic one-phase regions, which are normal (L_1) and inverse (L_2) micellar phases. Both are transparent, but the L_2 phase has a yellowish tinge due to the inherent color of THFM. The viscosity of the liquid crystalline phases at high surfactant concentrations prevents the exact determination of phase boundaries (dashed lines). There is a small three-phase region around the composition marked by the dot in Figure 1a. In this region, the more dense L_2 phase is in equilibrium with L_1 (middle phase) and L_α (upper phase).

Figure 1b is an expanded view of the water-rich corner of the phase diagram. The L_1 region shifts toward the water/AOT axis as temperature increases from 25 to 60 °C. The compositions of the o/w microemulsions polymerized are indicated in Figure 1b as full circles and squares. The unpolymerized microemulsions are fluid and are highly conductive (>1 mS/cm), suggesting water-continuous mi-

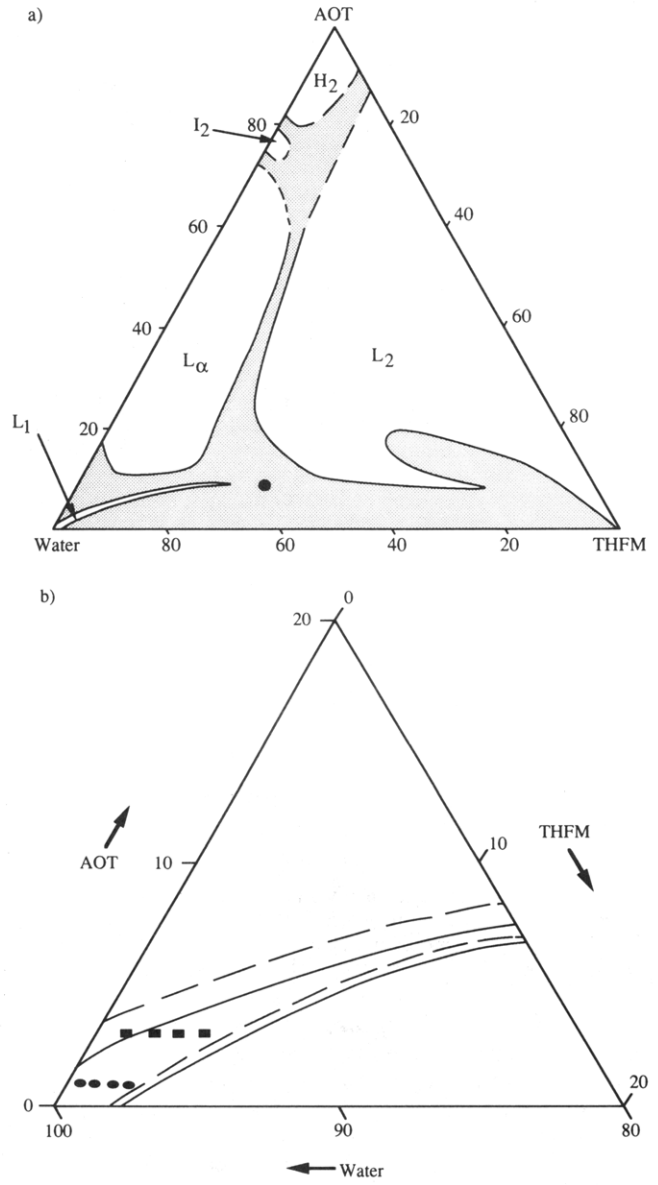

Figure 1. Phase behavior of AOT/water/THFM. (a) The entire phase diagram at 25 °C. The samples at high surfactant concentration are viscous and the boundaries were not determined exactly (dashed lines). One-phase regions are labeled as explained in the text. (b) Expanded view of the water-rich corner showing the boundaries of the microemulsion phase at 25 °C (solid lines) and 60 °C (dashed lines). The formulations polymerized along the AOT/water = 1/99 dilution path (circles) contain 0.5, 1.0, 1.5, and 2.0% (w/w) THFM, and those along the AOT/water = 3/97 dilution path (squares) contain 1.0, 2.0, 3.0, and 4.0% (w/w) THFM.

crostructures. QLS autocorrelation functions of an unpolymerized microemulsion containing 7.8% (w/w) THFM and 4.4% (w/w) AOT are single exponential with variances ν of about 0.1. The apparent diffusion coefficient is independent of q, consistent with the presence of spherical particles, and corresponds to diameters of about 4.5 nm.

Polymerization of these o/w microemulsions is fast, after an initial induction period. Conversions greater than 90% are achieved within 15–20 min (Figure 2). The initially transparent microemulsion becomes bluish as the reaction progresses. Final latexes are bluish-turbid to opaque depending on THFM and AOT concentrations in the parent microemulsions. Latexes originating from microemulsions with larger initial concentrations of monomer and surfactant are more turbid. The polymerization rate shows the two characteristic intervals observed before for

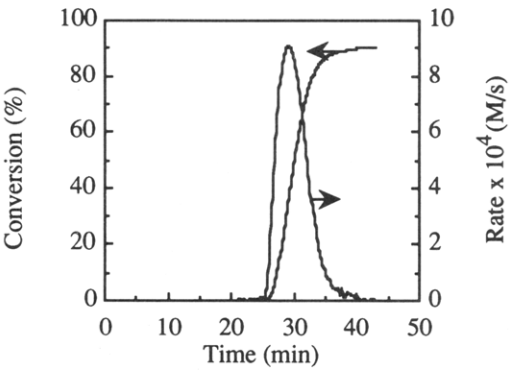

Figure 2. Conversion and rate data of the 3% (w/w) THFM and AOT/water = 3/97 microemulsion polymerized in the calorimeter.

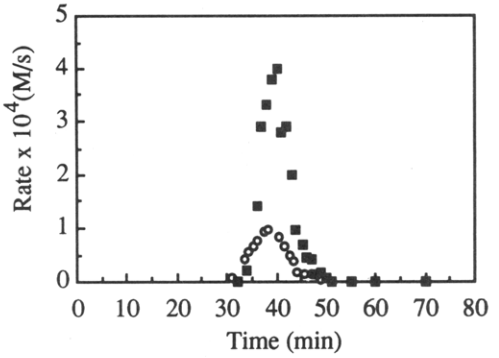

Figure 3. Rates of polymerization for parent microemulsions with 1% (w/w) THFM and AOT/water = 1/99 (circles) and 3% (w/w) THFM and AOT/water = 3/97 (squares). Rates were calculated from conversion data obtained by dilatometry.

Scheme I

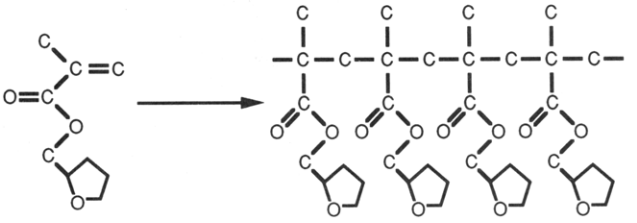

microemulsion polymerization:[6-8] an increasing rate interval followed by a decreasing rate interval. The maximum rate occurs at about 35–40% conversion, and the rate increases with initial THFM concentration (Figure 3). The enthalpy of polymerization of a 3% (w/w) THFM and 2.9% (w/w) AOT microemulsion determined by calorimetry is 14.9 kcal/mol. This enthalpy is in the range reported for other polymethacrylates derived from cyclohexyl methacrylate (12.7 kcal/mol), ethyl methacrylate (13.8 kcal/mol), butyl methacrylate (14.3 kcal/mol), *n*-hexyl methacrylate (14.8 kcal/mol), and 2-ethoxyethyl methacrylate (14.8 kcal/mol).[26] Although the reaction enthalpy is large and the reaction is rapid, all polymerization reactions were done under nearly isothermal conditions, so any increase of rate with temperature is minimal.

For polymer formation via a free radical mechanism, the C=C bond of the monomer reacts with the growing radical to form a chain with tetrahydrofurfuryl side groups (Scheme I). Direct evidence of this reaction is provided by in situ internal reflectance FTIR spectroscopy of the microemulsion as it polymerizes (Figure 4). The main spectral features in the 1800–900-cm^{-1} region are absorbance peaks at 1717 (vs), 1638 (w), 1458 (m), 1320 (sh), 1300 (s), 1171 (vs), 1081 (m), 1042 (m), 1023 (m), and 937 (w) cm^{-1}. Upon polymerization bands at 1638 and 937 cm^{-1}, due to the C=C stretch and the $=CH_2$ wag,

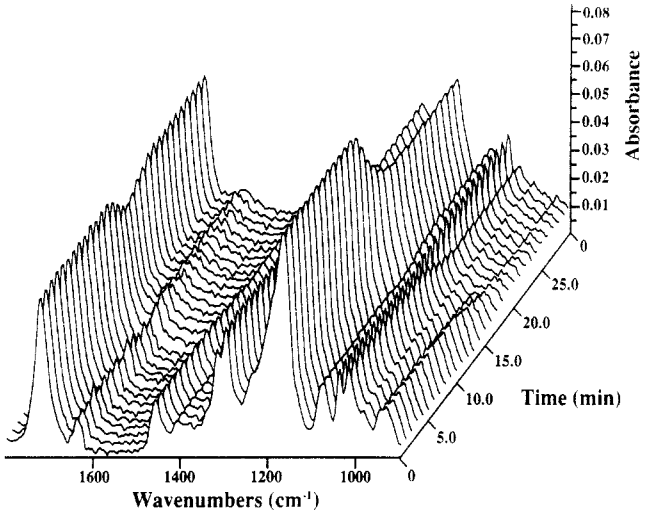

Figure 4. FTIR spectra of the 3% (w/w) THFM and AOT/water = 3/97 microemulsion during polymerization. Important spectral features of the polymerization are obscured by water absorbances; therefore, the spectrum of 1% (w/w) AOT in water was subtracted from these spectra to display the absorbance changes of monomer as it is converted to polymer.

Table I
Polymer Characteristics as a Function of Conversion

% conversion	intrinsic viscosity[a] $[\eta]$ (dL/g)	molecular weight[b] $\bar{M}_w$	polydispersity[b] $\bar{M}_w/\bar{M}_n$
3% (w/w) THFM Parent Microemulsion on 3/97 AOT/Water Dilution Path			
7.7	0.259	4 250 000	1.39
44.6	0.345	8 120 000	1.39
72.2	0.665	12 200 000	1.07
97.9	0.700	15 100 000	1.09
1% (w/w) THFM Parent Microemulsion on 1/99 AOT/Water Dilution Path			
97.5	1.192	7 020 000	1.17

[a] Intrinsic viscosities, at 30 °C in THF, measured by SEC DV detection. [b] Molecular weight (weight average) and polydispersity measured by SEC LALLS detection.

respectively, vanish with concomitant blue shift of the carbonyl band from 1717 to 1729 cm^{-1} due to loss of conjugation. Also, major changes occur in the cluster of bands found from 1350 to 1100 cm^{-1}. This cluster is primarily due to the backbone C—C stretching bands of the acid involving the C—O bond. Peaks at 1320 and 1300 cm^{-1} disappear, and the band at 1171 cm^{-1} becomes a broad doublet with peaks at 1237 and 1159 cm^{-1}. The unchanged bands at 1458 cm^{-1} are assigned to deformations of methyl or methylene ring groups while the unchanged bands at 1081 and 1042 cm^{-1} are related to the tetrahydrofurfuryl alcohol group.[27,28]

Polymer structure and particle growth were investigated by QLS and SEC as the reaction progressed. Because a fraction of the molecular weight ($\bar{M}_w$) distribution of the polyTHFM samples is near the column set exclusion limit (approximately 2 730 000 polystyrene $\bar{M}_w$) of the SEC column, absolute weight-average molecular weights ($\bar{M}_w$), were obtained by integrating the response of the LALLS detector. Table I reports intrinsic viscosity $[\eta]$, $\bar{M}_w$, and polydispersity ($\bar{M}_w/\bar{M}_n$) as a function of conversion of the polymerization of a 3% (w/w) THFM and 3% (w/w) AOT microemulsion.

Analysis of scattering from strongly interacting systems such as ionic microemulsions is difficult.[19] However, the normalized intensity autocorrelation functions for undiluted reacting samples, even at low conversion (1%), are

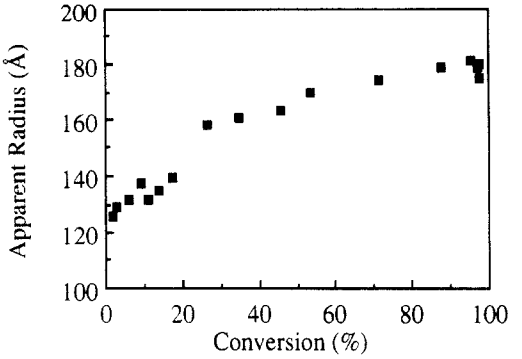

Figure 5. Apparent size of the polymer particle as a function of conversion for the polymerization of a 1.0% (w/w) THFM and AOT/water = 1/99 microemulsion. Conversion was determined by gravimetry and the sizes were estimated from QLS measurements of undiluted samples.

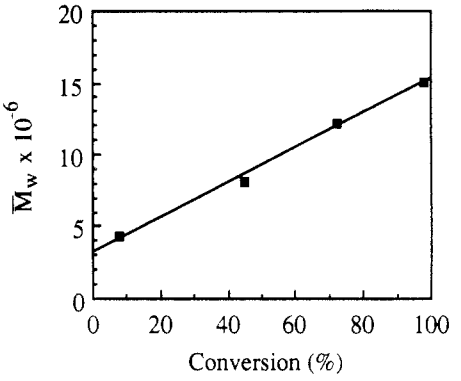

Figure 6. Polymer molecular weight as a function of THFM conversion for polymerization of a 3.0% (w/w) THFM and AOT/water = 3/97 microemulsion. Conversion was determined by gravimetry and the molecular weights by LALLS.

single-exponential decay functions with small values of variance, $\nu < 0.05$; i.e., only one apparent size is observed after the system begins to polymerize. The apparent diffusion coefficients are independent of q, which suggests the particles are spherical. Polymer particles grow steadily as the reaction proceeds (Figure 5), and the molecular weight increases concurrently (Figure 6). The values of $\bar{M}_w$ are enormous even at low conversions (see Table I). Both these results indicate fast reaction rates and particle growth as the reaction proceeds.

The values of $\bar{M}_w$ and of particle size, assuming that the density of the particles is that of bulk polymer (1.222 g/cm^3),[29] suggest that each particle contains only one or a few macromolecules. Polydispersity is low in all cases (1.07–1.39). The values of $[\eta]$, obtained by integration of the SEC DV detector response, are consistently lower than those of linear polystyrene of similar molecular weights, indicating a large degree of branching. Plots of log $[\eta]$ vs SEC retention volumes are usually close to linear for homogeneous branched materials. However, similar plots for the eluted fractions of the polyTHFM produced here deviate significantly from linearity, suggesting that the branching is heterogeneous across the molecular weight distribution.

Latexes were produced from parent microemulsions of different compositions using identical reaction conditions: four along the AOT/water = 1/99 dilution path and four along the AOT/water = 3/97 dilution path (see Figure 1b). Final particle size increases linearly with THFM concentration in the parent microemulsions when the AOT/water ratio is held constant (Figure 7). All polymerized microemulsions appear bluish. However, the 1/99 latexes are translucent and remain stable for days, whereas the 3/97

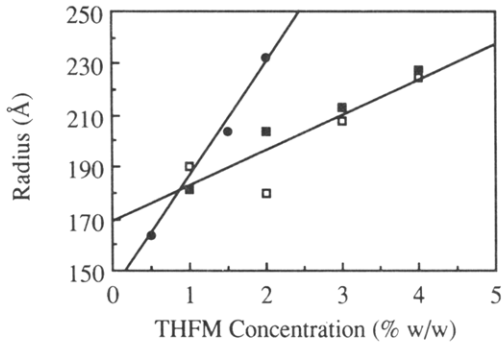

Figure 7. Final particle size as a function of the initial composition of the microemulsion. Radii were measured by QLS using samples diluted 500 times with water (solid circles and solid squares). The sizes corresponding to z-average diffusion coefficients were obtained by image analysis of transmission electron micrographs (open squares). Circles and squares correspond to latexes derived from parent microemulsions with AOT/water = 1/99 and AOT/water = 3/97, respectively.

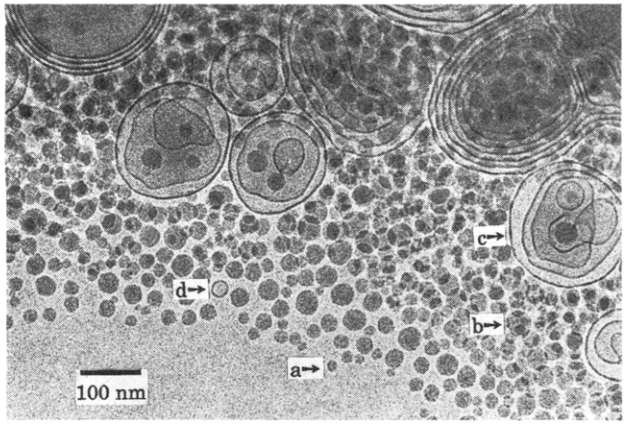

Figure 8. Transmission cryoelectron micrograph of the 3% (w/w) THFM and AOT/water = 3/97 microemulsion after polymerization. This direct image was obtained through a bioconcave thin film, vitrified cryogenically as described in the text. The small, dark circles (a) are polyTHFM particles. In thicker regions of the film, overlapping particles (b) are evident. The network of dark lines (c) corresponds to excess AOT organized into dispersed lamellar structures. The smallest of these structures (d) is similar in size to the polymer particles. The larger structures illustrated include a variety of manifestations of the lamellar liquid crystalline mesophase.

latexes are turbid, flocculate, and sediment after 1 day. TEM micrographs of the polymerized 3/97 samples show two coexisting microstructures: spherical particles with diameters of 15–50 nm and lamellar and multilamellar structures with 9-nm interbilayer spacing (see tetralamellar structure in upper left corner of Figure 8). The interbilayer spacings are consistent with those reported for the AOT/water lamellar phase.[30]

The particle size distributions, obtained by image analysis of the TEM micrographs, show that the particles are polydisperse but the average size increases with THFM concentration of the unpolymerized microemulsion (Figure 9). These distributions yield first moments (mean diameters) of 25, 25, 28, and 34 nm, respectively, for 1, 2, 3, and 4% (w/w) THFM formulations. A z-average diameter ($\bar{d}_z$, which is the sixth moment of the distribution normalized by the fifth moment and is derived from the definition of the molecular weight z-average assuming a uniform polymer density) calculated from the particle size distributions agree closely with the QLS results shown in Figure 7.

THFM was also polymerized at 60 °C in aqueous solution, in toluene solution, and in an emulsion (1% AOT, 9.9% THFM, and 89.1% water). In the first case, 0.5% (w/w) THFM aqueous transparent solutions were initiated at 60 °C with potassium persulfate or AIBN (1% (w/w) with respect to monomer) to produce stable, milky, and opaque latexes containing particles of about 160 and 230 nm in diameter, respectively. In either case, the dried polymer cannot be dissolved in solvents such as THF and toluene, suggesting that the polymer is cross-linked. A 7.5% (w/w) THFM solution in toluene was polymerized at 60 °C using AIBN as initiator. The final solution was transparent and slightly viscous, and the isolated polymer was soluble in THF and toluene, indicating very little or no cross-linking. In the case of emulsion polymerization initiated with potassium persulfate, the reaction rate at 60 °C is fast (10–15 min) and the final product is a milky latex containing particles of about 57 nm in diameter. The dried polymer is cross-linked since it does not dissolve in any solvent.

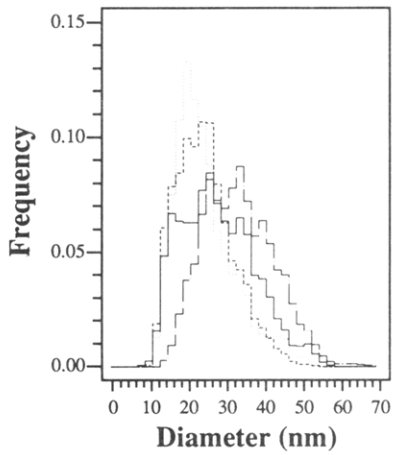

Figure 9. Particle size distributions determined by image analysis of transmission cryoelectron micrographs of polymerized microemulsions along the AOT/water = 3/97 dilution path. These are normalized number density distributions and correspond to different amounts (w/w) of THFM in the parent microemulsion before polymerization: 1% (···), 2% (- - -), 3% (—), 4% (– · –).

Discussion

The phase behavior of the THFM system is similar to other AOT/oil/water ternary systems.[31,32] The same number and types of one-phase regions are located in the same relative positions on the Gibb's triangle, and the inverse surfactant L_2 phase dominates the phase behavior (Figure 1). AOT forms inverse phases because its packing parameter, $v/l_c a$, is near 1,[33,34] where v is the volume occupied by hydrocarbon tails, a is the effective area of head groups at the interface, and l_c is the length of hydrocarbon tails. An unusual feature of the THFM phase diagram is the protrusion of the two-phase region near the oil-rich corner into the L_2 region, which requires the coexistence of an AOT-rich L_2 phase with an AOT-poor L_2 phase. The L_1 region (Figure 1b) is also much larger than those reported in other AOT ternary systems.[31] Both of these features are the result of the high solubility of THFM in water (0.8%) and the polar nature of the tetrahydrofurfuryl ring.

The structure of dilute AOT solutions in D_2O was studied by Sheu et al.[35] using small-angle neutron scattering. They found spherical micelles of 2.5 nm in diameter with an aggregation number of 15 at the critical micelle concentration (cmc) and showed that the micelles become oblate as the AOT concentration increases. Presumably, the introduction of oil into the micelle core releases the constraint of the tails reaching to the center and allows

alternative micelle geometries. The size and shape of the swollen micelles depends on the properties of the oil.[34] For a microemulsion containing 4.4% (w/w) AOT and 7.8% (w/w) THFM, TEM shows swollen spherical micelles of 5 nm in diameter,[15] in excellent agreement with the QLS measurements of spherical particles of 4.5 nm in diameter. Insertion of THFM molecules into the AOT surfactant layer apparently reduces the monolayer rigidity, and allows the formation of spherical swollen micelles. Reducing the THFM content of L_1 samples while maintaining a constant AOT/water ratio leads to the formation of L_α, a phase of zero surfactant monolayer curvature (see Figure 1). THFM acts not only as the hydrophobic component but also as a cosurfactant, much as acrylamide does in AOT/water/toluene w/o microemulsions.[9]

The transparent microemulsions become increasingly turbid as polymerization proceeds, indicating the growth of particles and the formation of lamellar structures. The onset of polymerization, which is signaled by a turbidity increase, does not occur immediately after injection of the initiator. This induction period is likely caused by impurities (or oxygen) that scavenge initiator radicals,[1] and the length of the induction period depends on the efficiency of sparging. After the reaction begins, THFM polymerizes much more rapidly than does styrene in a microemulsion formulation.[7] Conversions greater than 90% are achieved within 15 min after the induction period (Figure 2), while conversions of only 70–90% are obtained after 120 min of reaction for DTAB/water/styrene microemulsions at identical temperatures and $K_2S_2O_8$ concentrations. The activation energies for the emulsion polymerizations of methyl methacrylate (22.4–29.4 kJ/mol) are smaller than those found for styrene emulsion polymerizations (29.0–59.0 kJ/mol).[16] Although the smaller activation energies of methyl methacrylate would explain the faster reaction rates, consideration of the size and number of swollen micelles, the monomer concentration in the swollen micelles, and the solubilities and diffusion coefficients of monomers in water is required when a time-dependent expression for monomer consumption during microemulsion polymerization is developed.[36]

The polymerization rates vs conversion curves (Figures 2 and 3) show only two rate intervals in contrast to the three intervals observed in emulsion polymerization.[1] In the first interval, the polymerization rate increases with time since the number of propagation sites increases. During this interval the diffusive transport of monomer from uninitiated droplets maintains a constant monomer concentration in the growing polymer particles. The nucleation interval ends when all the uninitiated droplets have been depleted of monomer. Since the uninitiated monomer-swollen micelles are no longer available, the concentration of monomer within each particle steadily decreases as the reaction proceeds, and the polymerization rate in the second interval slows. As in other microemulsion polymerizations, no Trommsdorff or gel effect was observed.[6,7] An increase in the maximum rate as the initial monomer concentration increases (Figure 3) is consistent with the hypothesis that the reaction rate depends on the number of polymerizing loci. Similar results have been reported for styrene microemulsion polymerization.[6-8] For THFM, the maximum rate occurs at approximately 35–40% conversion, while styrene microemulsion polymerization has a maximum rate at about 20% conversion.[6-8]

FTIR spectra show the progress of THFM polymerization. The disappearance of the IR absorbances associated with the C=C bond (Figure 4) indicates that

Scheme II

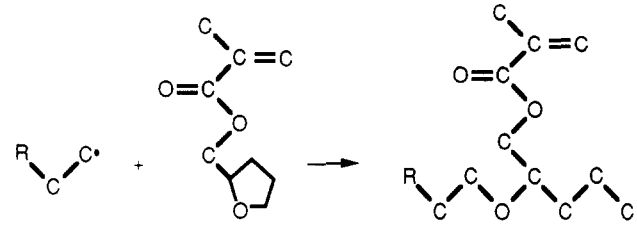

propagation occurs through the methacrylate moiety (Scheme I). In addition to the free radical mechanism for monomer addition, cross-linking involving the opening of the tetrahydrofurfuryl ring may also occur (Scheme II). Typically, cationic and anionic initiators are used in the ring-opening polymerization of heterocyclic ethers such as THF.[37] However, Patel et al.[38] reported a free-radical ring-opening of heterocyclic methacrylates. The degree of cross-linking, as determined by polymer solubility in THF, appears to depend on the type of initiator and the solvent environment. Free radical polymerization, either in bulk[38] or in aqueous solution yields a cross-linked polymer that is insoluble in any solvent, but fewer than 1% of the monomer units are apparently involved in cross-linking and hence in ring-opening reactions.[38] Redox-initiated microemulsion polymerization of THFM also results in a cross-linked polymer.[15]

The polyTHFM produced here is soluble in THF and other solvents; thus the polymer is not cross-linked, although probably highly branched (see below). Evidently, a hydrophobic environment, whether it is the micelle interior in microemulsion polymerizaton or the organic nonpolar solvent (such as toluene) in solution polymerization, is less conducive to free-radical ring opening reactions than an aqueous environment. The insertion of tetrahydrofurfuryl groups into the AOT surfactant layer could also provide protection from ring-opening reactions. Solubilization of THFM in AOT offers no protection when redox initiation is used,[15] probably because ionic species are produced that are more likely to induce ring-opening reactions.[37]

Particles grow during most o/w and w/o microemulsion polymerizations.[4,7,14] Here particle growth was followed by QLS and SEC (Figures 5 and 6). Measurement of the actual particle size by QLS in reacting microemulsions is complicated by the influence of interparticle interactions,[19] but the *apparent* size increases as the reaction proceeds (Figure 5). Measuring particle growth by SEC is also difficult because of the high molecular weights ($(4–15) \times 10^6$) obtained here. Although complete molecular weight distributions cannot be measured, considerable information can be obtained from the response of the various SEC detectors.[21,39,40] Molecular size in THF, estimated from the peak apex of the DRI response and calculated values of polystyrene standards that elute at the same retention volume, increases with conversion. Polydispersity ($\bar{M}_w/\bar{M}_n$) can be approximated from the LALLS response without dependence on calibration curves and complications associated with the mole fraction of polymer eluting near the exclusion limit of the SEC column set. Both polydispersity indexes ($\bar{M}_w/\bar{M}_n = 1.07–1.39$) and particle size distributions are relatively narrow throughout the entire polymerization process. Absolute molecular weights determined by integrating the total LALLS intensity also increase monotonically with conversion (Figure 6).

The increase in both molecular weights (SEC) and apparent sizes (QLS) provide conclusive evidence of particle growth during polymerization. Further, the apparently small particle sizes and large molecular weights

suggest that the polymer chains are collapsed and that only one, or at most several, macromolecules make up each particle. A similar small number of polymer chains per particle has been reported for w/o polymerization of acrylamide[9] and for o/w polymerization of styrene.[6] Extrapolation of $\bar{M}_w$ to 0% conversion corresponds to a particle diameter of 20 nm, assuming that each particle contains only one macromolecule and the density of the polymer molecule is 1.22 g/mL. It is apparent, in reviewing the size distributions in Figure 9 for latexes derived from microemulsions of varying THFM content, that the smallest size "mode" is approximately 20 nm in all four cases illustrated. We hypothesize at this stage that this 20-nm mode, which coincidentally corresponds to the intercept in Figure 6, occurs because the kinetic mechanisms that determine chain growth are competitive with the mass transport mechanisms that determine the availability of monomer, oligomeric free-radicals, and other pertinent species. The final size a latex particle achieves is thus a consequence of the interplay of polymerization kinetics (initiation, propagation, and termination) and the diffusion of these species through the aqueous continuum. The feasibility of this hypothesis will be tested in a future publication.

The comparison of the molecular weight of the polyTHFM with linear polystyrene standards of equivalent hydrodynamic sizes suggests that polyTHFM is highly branched. The intrinsic viscosity of polyTHFM is lower than those of the linear polystyrene standards, which is consistent with the presence of highly branched polymers. Branching can be caused by chain-transfer reaction to polymer and monomer in free-radical polymerization.[41] The rate constants for chain-transfer reactions to polymer for THFM are not known, but reported rate constants for methyl methacrylate polymerization are large.[16]

TEM micrographs of the polymerized microemulsions with concentrations along the 3/97 dilution path show the polymer particles as well as lamellar structures (Figure 8). The interbilayer spacing of these structures is similar to the Bragg spacing of the lamellar phase reported for AOT/water lamellar phase (between 2.8 and 12.8 nm depending on AOT concentration).[30] The in situ formation of these lamellar structures as polymerization progresses is a consequence of the low AOT concentration required to form a lamellar phase in water (1.4% (w/w) at 25 °C)[30] and the drastic reduction in interfacial area as particles grow. Hence, when the concentration of AOT, the majority of which is originally located at the surface of swollen micelles but is expelled as polymerization proceeds, exceeds the solubility limit, lamellar liquid crystallites form. This is supported by observations of latex stability. Latex synthesized from microemulsions along the 1/99 AOT/water dilution path are bluish-translucent and remain stable for months. In contrast, the lamellar crystallites in latexes produced along dilution lines of 3/97 tend to flocculate and sediment. The sediment is not made of coalesced polymeric particles, but is a loosely flocculated lamellar phase, which readily dissolves upon dilution with water.

Final particle sizes, as determined by QLS measurements of extremely dilute dispersions, depend on the concentrations of THFM and AOT in the parent microemulsions (Figure 7). Increasing the amount of THFM at constant surfactant/water ratio results in larger latex particles. This effect is more dramatic for smaller surfactant/water ratios. Increasing the amount of surfactant yields smaller particles in the latex because increasing the surfactant/water ratio results in more sites to distribute monomer. QLS indicates that the latexes contain nearly monodisperse, spherical particles. TEM of the polymerized microemulsion confirmed that the particles are spherical and that they range in diameters from 15 to 50 nm. The presence of a distribution suggests that propagation sites are continuously formed during interval *I*. The size distributions corroborate the QLS data and show that increasing initial monomer concentration leads to increasing particle sizes (Figure 7). The dynamic QLS experiment is more sensitive to the largest particles in the latex, whereas the TEM distributions sample the breadth of the particle sizes more uniformly.

These findings lead to the following hypothesis: After propagation sites have been formed, radicals generated in the aqueous phase diffuse toward these sites and initiate (or terminate) chain propagation. As the polymer chain grows during interval *I*, monomer concentration in the initiated micelle is maintained by diffusion from uninitated micelles. The adsorption of the monomer at the interface increases monomer stability, and probably enhances the polymerization rate. As the particle size increases, the total interfacial area of the polymerizing microemulsion decreases, and excess AOT forms the same type of structures that occur in binary mixtures of AOT and water.

Conclusions

Polymerization of transparent oil-in-water microemulsions of AOT, water, and THFM produces monodisperse stable latexes containing particles with mean diameters of 25–34 nm depending on surfactant and monomer concentrations in the parent microemulsion. Polymer molecular weights are high even at low conversions (4.25×10^6 at 7.7% conversion) and increase linearly as the reaction proceeds. Apparent particle size also increases with increasing conversion. The large molecular weights and small particle size demonstrate that each particle contains only one, or at most several, polymer molecules. These findings support the hypothesis that in microemulsion polymerization, latex particles, after their formation, recruit monomer from uninitiated droplets. AOT from the monomer-depleted micelles forms disperse lamellar and multilamellar microcrystallites when the AOT concentration exceeds its solubility limit in water (1.4% w/w).

Acknowledgment is made to the donors of the Petroleum Research Fund, administered by the American Chemical Society, to CONCAyT (Grant P228CCOX-881263) and the Secretaria de Educación Pública de México (Grant DGICSA 901637), to Spectra-Tech, Applied Systems Division, and to the Center of Catalytic Science and Technology at the University of Delaware. We thank Sally M. Miller, Harold Wolcott, and Peter Ghyzel for their assistance in molecular weight characterization, gas chromatographic analysis, and calorimetry, respectively.

References and Notes

(1) Piirma, I. *Emulsion Polymerization*; Academic Press: New York, 1976.

(2) Chamberlain, B. J.; Napper, D. H.; Gilbert, R. G. *J. Chem. Soc., Faraday Trans. 1* **1982**, *78*, 591.

(3) Choi, Y. T.; El-Aasser, M. S.; Sudol, E. D.; Vanderhoff, J. W. *J. Polym. Sci., Polym. Chem. Ed.* **1985**, *23*, 2973.

(4) Candau, F. In *Encyclopedia of Polymer Science and Engineering*; Mark, H. F., Bikales, N. M., Overberger, C. G., Menges, G., Eds.; John Wiley: New York, 1987; Vol. 9.

(5) Stoffer, J. O.; Bone, T. *J. Dispersion Sci. Technol.* **1980**, *1*, 37; *J. Polym. Sci., Polym. Chem. Ed.* **1980**, *18*, 2641.

(6) Guo, J. S.; El-Aasser, M. S.; Vanderhoff, J. W. *J. Polym. Sci., Polym. Chem. Ed.* **1989**, *27*, 691.
(7) Puig, J. E.; Pérez-Luna, V. H.; Pérez-González, M.; Macías, E. R.; Rodríguez, B. E.; Kaler, E. W. *Colloid Polym. Sci.*, in press.
(8) Gan, L. M.; Chew, C. H.; Lye, I.; Imae, T. *Polym. Bull.* **1991**, *25*, 193.
(9) Candau, F.; Leong, Y. S.; Pouyet, G.; Candau, S. *J. Colloid Interface Sci.* **1984**, *101*, 167.
(10) Candau, F.; Leong, Y. S.; Fitch, R. M. *J. Polym. Sci., Polym. Chem. Ed.* **1985**, *23*, 193.
(11) Haque, E.; Qutubuddin, S. *J. Polym. Sci., Polym. Lett. Ed.* **1988**, *26*, 429.
(12) Murtagh, J.; Ferrick, M. R.; Thomas, J. K. *Polym. Prepr., Am. Chem. Soc. Div. Polym. Chem.* **1987**, 28, 441.
(13) Vinson, P. K.; Bellare, J. R.; Davis, H. T.; Miller, W. G.; Scriven, L. E. *J. Colloid Interface Sci.* **1991**, *142*, 74.
(14) Pérez-Luna, V. H.; Puig, J. E.; Castaño, V. M.; Rodríguez, B. E.; Murthy, A. K.; Kaler, E. W. *Langmuir* **1990**, *6*, 1040.
(15) Texter, J.; Oppenheimer, L.; Minter, J. R. *Polym. Bull.* **1992**, *27*, 487.
(16) Brandrup, J.; Immergut, E. H. *Polymer Handbook*; John Wiley: New York, 1989.
(17) Maitra, A. N.; Eicke, H.-F. *J. Phys. Chem.* **1981**, *85*, 2687.
(18) Gan, L. M.; Chew, C. H.; Friberg, S. E. *J. Macromol. Sci. Chem.* **1983**, *A19*, 739.
(19) Chang, N. J. Ph.D. Thesis, University of Washington, 1986.
(20) Mourey, T. H.; Miller, S. M. *J. Liq. Chromatogr.* **1990**, *13*, 693.
(21) Mourey, T. H.; Miller, S. M.; Balke, S. T. *J. Liq. Chromatogr.* **1990**, *13*, 435.
(22) Bellare, J. R.; Davis, H. T.; Scriven, L. E.; Talmon, Y. *J. Electron Microsc. Technol.* **1988**, *10*, 87.
(23) Fukami, A.; Adachi, K. *J. Electron Microsc.* **1965**, *14*, 112.
(24) Dubocher, J.; Lepault, J.; Freeman, R.; Berriman, J. A.; Homo, J.-C. *J. Microsc.* **1982**, *128*, 219.
(25) Rosevear, F. B. *J. Soc. Cosmet. Chem.* **1968**, *19*, 581.
(26) Lee, H.; Colby, C. *Dent. Mater.* **1986**, *2*, 175.
(27) Pouchart, C. J. *The Aldrich Library of Infrared Spectra*; Aldrich Chemical Co., Inc.: Milwaukee, WI, 1981.
(28) Colthup, N. B.; Daly, L. H.; Wilberley, S. E. *Introduction to Infrared and Raman Spectroscopy*; Academic Press: Boston, 1990.
(29) Patel, M. P.; Braden, M.; Davy, K. W. M. *Biomaterials* **1987**, *8*, 53.
(30) Fontell, K. *J. Colloid Interface Sci.* **1973**, *44*, 318.
(31) Ekwall, P.; Mandell, L.; Fontell, K. *J. Colloid Interface Sci.* **1970**, *33*, 215.
(32) Eicke, H.-F.; Markovic, Z. *J. Colloid Interface Sci.* **1981**, *79*, 151.
(33) Isrealachvili, J. N. *Intermolecular and Surface Forces*; Academic Press: London, 1985.
(34) Israelachvili, J. N.; Mitchell, D. J.; Ninham, B. W. *J. Chem. Soc., Faraday Trans. 1* **1976**, *72*, 1525.
(35) Sheu, E. Y.; Chen. S.-H.; Huang, J. S. *J. Phys. Chem.* **1987**, *91*, 3306.
(36) Min, K. W.; Ray, W. H. *J. Macromol. Sci. Rev. Macromol. Chem.* **1974**, *C11*, 177.
(37) Inuoe, S.; Aida, T. In *Ring-Opening Polymerization*; Ivin, K. J., Saegusa, T., Eds.; Elsevier Applied Science Publishers: New York, 1984; Vol. 1.
(38) Patel, M. P.; Braden, M. *Biomaterials* **1989**, *10*, 277.
(39) Mourey, T. H.; Turner, S. R.; Rubinstein, M.; Frechet, J. M. J.; Hawker, C. J.; Wooley, K. *Macromolecules* **1992**, *25*, 2401.
(40) Mourey, T. H.; Miller, S. M.; Wesson, J. A.; Long, T. E.; Kelts, L. W. *Macromolecules* **1992**, *25*, 45.
(41) Odian, G. *Principles of Polymerization*; Wiley: New York, 1981.

Registry No. THFM, 2455-24-5; THFM (homopolymer), 25035-85-2; AOT, 577-11-7.